CHIN. PHYS. LETT. Vol. 36, No. 12 (2019) 124202

Photoexcited Blueshift and Redshift Switchable Metamaterial Absorber at Terahertz Frequencies *

Zong-Cheng Xu(续宗成)[1,2]**, Liang Wu(吴亮)[2], Ya-Ting Zhang(张雅婷)[2], De-Gang Xu(徐德刚)[2], Jian-Quan Yao(姚建铨)[2]

[1]*Department of Physics, Tianjin University Renai College, Tianjin 301636*

[2]*Institute of Laser and Opto-electronics and Key Laboratory of Opto-electronics Information Science and Technology (Ministry of Education), Tianjin University, Tianjin 300072*

(Received 19 July 2019)

We propose a design and numerical study of an optically blueshift and redshift switchable metamaterial (MM) absorber in the terahertz regime. The MM absorber comprises a periodic array of metallic split-ring resonators (SRRs) with semiconductor silicon embedded in the gaps of MM resonators. The absorptive frequencies of the MM can be shifted by applying an external pump power. The simulation results show that, for photoconductivity of silicon ranging between 1 S/m and 4000 S/m, the resonance peak of the absorption spectra shifts to higher frequencies, from 0.67 THz to 1.63 THz, with a resonance tuning range of 59%. As the conductivity of silicon increases, the resonance frequencies of the MM absorber are continuously tuned from 1.60 THz to 1.16 THz, a redshift tuning range of 28%. As the conductivity increases above 30000 S/m, the resonance frequencies tend to be stable while the absorption peak has a merely tiny variation. The optical-tuned absorber has potential applications as a terahertz modulator or switch.

PACS: 42.25.Bs, 78.20.Ci, 41.20.Jb DOI: 10.1088/0256-307X/36/12/124202

Metamaterials using artificial designed “atoms" to create an electric or magnetic response to incident electromagnetic radiation exhibit notable properties (which are unavailable with naturally occurring materials) within a wide range of frequencies from microwaves towards visible regions, especially to operate at terahertz frequencies.[1–4] The terahertz technique has attracted great attention for its potential applications in communications, security and biotechnology.[5–7] Therefore, there has been increasing interest in THz microstructured devices, such as filters, absorbers and sensors.[8–11] Metamateral (MM) absorber is a novel device to provide near unity absorption to electromagnetic wave, which is usually constructed by patterning a metallic layer over another metallic layer spaced by a dielectric layer. In 2008, Landy *et al.* first experimentally demonstrated a perfect MM absorber to absorb all incident radiation in microwave bands, which was composed of a sandwiched structure of electric ring resonators, di-electric substrate, and metal cut-wires.[12] Since then, multiband or broadband MM absorbers employing multilayered or unit cells containing structures resonating at different frequencies have been proposed and investigated widely.[13–17] Recently, there has been considerable interest in the realization of frequency-agile functionality provided by passive tuning based on integrating a natural reconfigurable material and applying an external stimulus to achieve tuning. For example, MMs can be tuned by doping graphene[18–20] through external voltage control to achieve the amplitude modulation or the spectral tuning.[21–24] Another approach of tunability was confirmed using thermal control, which is based on a variation of temperature altering the intrinsic carrier density in a semiconductor (InSb).[25,26] In addition, a thermally induced insulator-metal phase transition in vanadium dioxide was also employed to develop active MMs.[27,28] By integrating semiconductors into MM designs, a blueshift tunability MM through photoexcited carrier injections was realized in Ref. [29]. The tuning can be implemented within quite a broad frequency range of as much as 40%. Recently, the concept of coding MMs was proposed to realize various manipulations.[30,31] In our previous work, we presented an demonstration of optically blueshift tunable perfect terahertz MM absorber.[32] We also proposed a design and numerical study of an optically switchable MM absorber in a terahertz regime.[33]

In this Letter, we report an optically switchable MM absorber by inserting photoconductive silicon within the two gaps of split-ring resonators in the THz region, although it is difficult to find naturally occurring materials with very strong absorption.[28] We numerically demonstrate that a composite structure of a metallic split-ring resonator with semiconductor silicon embedded in the gaps of MM resonators, a lossy polyimide separation layer, and a metal ground film can be used as an effective tunable absorber. The switchable MM absorber is realized by their coupling with semiconductors and by tuning the semiconductors' conductivity. We demonstrate that a blueshift

*Supported by the National Key Research and Development Program of China under Grant No. 2017YFA0700202.

**Corresponding author. Email: zongchengxu78@163.com

© 2019 Chinese Physical Society and IOP Publishing Ltd

switch of the absorption peak frequency can be dynamically tuned from 0.67 to 1.63 THz, with a broadband tuning range of 59%. The working frequency of the MM resonant absorber is demonstrated to be continuously tuned from 1.60 to 1.16 THz by further increasing photoconductivity of silicon, with a broadband redshift tuning range on the order of 28%. The optical-tuned absorber provides a promising path towards the development a new class of MM devices and has potential applications as a terahertz modulator or switch.

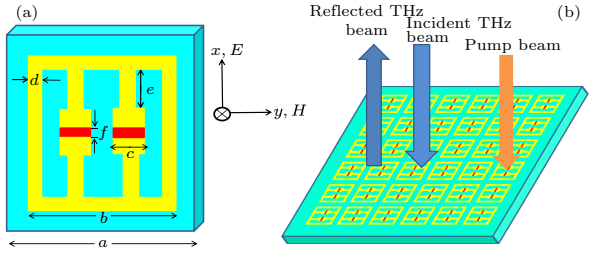

Fig. 1. (a) The unit cell of the MM absorber structure. The yellow regions are gold, the red region is photosensitive semiconductor silicon, and the light green region is the dielectric polyimide. The axes indicate the polarization and propagation direction of the incident THZ wave (E, H and K represent the electric field, magnetic field, and wave vector, respectively). (b) Perspective of a planar array. The pump power of THz wave is incident normally on the planar array.

The MM absorber has three layers: a square array consisting of two single hybrid split rings resonators (SRRs) with embedded semiconductor silicon in the gaps, a polyimide dielectric separation layer and a gold ground plane. Figure 1(a) shows the unit cell of the MM tunable absorber, as well as the propagation direction of the incident electromagnetic (EM) wave. The thickness of the metallic particle and ground plane is 200 nm, with a frequency-independent conductivity $\sigma_{\text{gold}} = 4.09 \times 10^7\,\text{S/m}$. The thicknesses of the dielectric separation layer is 12.3 μm, with dielectric constant[34] $\varepsilon = 2.9$ and loss tangent $\tan(\delta) = 0.02$.[32] The lattice constant of the tunable MM absorber is $a = 61\,\mu\text{m}$ and other geometric parameters $b = 53\,\mu\text{m}$, $c = 9\,\mu\text{m}$, $d = 3\,\mu\text{m}$, $e = 18\,\mu\text{m}$, $f = 4\,\mu\text{m}$. Photoconductive silicon (red part) is put in the gaps of the gold SRRs. The photoconductive silicon is simulated with $\sigma_{\text{Si}} = 11.7$. To simulate the photoconducting semiconductor response, we use different values of conductivity to reflect the different levels of photoexcitation, as a result of different values of an applied pump power. By incorporating photoconductive silicon into the MM absorber, a tunable resonance absorption mode switchable is achievable. We model its absorption spectrum using the commercial software CST Microwave Studio 2010. In our simulations, the periodic boundary conditions are used and the polarizations of the incident electromagnetic wave are set with the electrical field y-polarized and magnetic field x-polarized, in which the wave vector is perpendicular to the absorber plane. The polarization of the incident wave's electric field is perpendicular to the split gaps. Figure 1(b) shows the period arrays of unit cell. Absorptivity is defined as $A(\omega) = 1 - R(\omega) - T(\omega)$, $R(\omega) = |S_{11}|^2$ and $T(\omega) = |S_{21}|^2$, where $R(\omega)$ and $T(\omega)$ are the reflectance and transmittance, respectively. The reflection and transmission can be obtained from the frequency-dependent S-parameter in the simulation. Clearly, the higher performance of an absorber is equivalent to minimizing the reflectance and transmittance, in which the transmittance $T(\omega) = 0$ in the entire investigated frequency range due to the presence of the gold ground plane. Therefore, the absorbance can be maximized by inducing the reflectance.

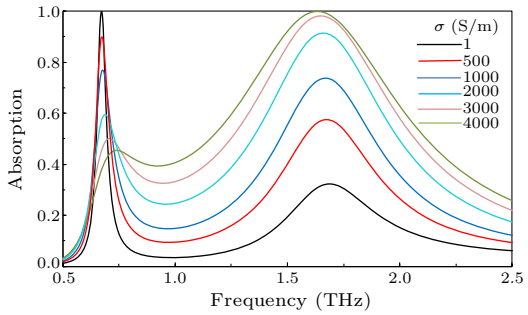

Fig. 2. Simulated absorption spectrum of the proposed MM absorber for different values of silicon conductivity.

When optical radiation is incident on the semiconductor silicon, an excessive carrier density is generated as long as the energy of light exceeds the band gap energy of the semiconductor. The photo-induced carriers can be considered as an electron-hole plasma and taken to be proportional to the fluence of incident photons. Filing the gap between the resonator arm with a semiconductor (silicon) leads to easy modification of its optical response through a pump beam which changes conductivity of Si. The conductivity of silicon is a function of incident pump power. Therefore, the conductivity of silicon is tuned effectively by applying an external pump power. In this study, we assume that the pump beam is near-infrared laser pulses with a central wavelength of 800 nm and a repetition rate of 1 kHz to optically excite charge carriers across the 1.12 eV bandgap of silicon. The lifetimes of photogenerated carriers in semiconductor silicon is about a few hundreds of nanoseconds, which is much longer than the picosecond duration of the THz pulses. The temporal delay between the optical pump and the THz beam can ensure a quasisteady state for the charge carriers of silicon. It is possible to adjust the conductivity of the silicon by changing the pump laser power. Figure 2 shows the simulated absorption spectra for different silicon conductivities. It can be seen clearly that the corresponding absorption of nearly unity (99.8%) is achieved at 0.67 THz without illumination. With the increase of silicon conductivity,

the increasing photoexcited charge carriers in the gap make the resonance weaker, resulting in a decrease of absorption, and accompanied by a blueshift of the absorption peak frequency. As the conductivity increases to $\sigma_{\rm Si} = 4000\,{\rm S/m}$, the absorption strength is enhanced again and reaches another absorption peak at 1.63 THz with 100% absorption.

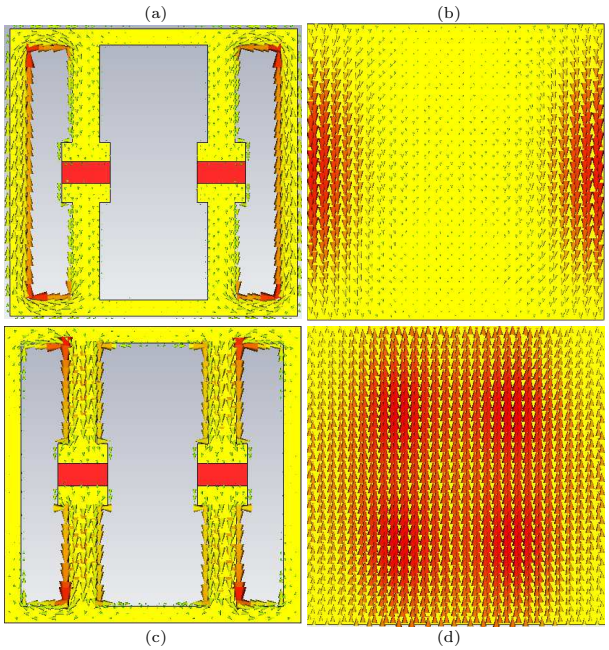

Fig. 3. The simulated absorption of the calculated surface current density for (a) and (b) the lower-frequency absorption at 0.67 THz for $\sigma_{\rm Si} = 1\,{\rm S/m}$, (c) and (d) the higher-frequency absorption at 1.63 THz for $\sigma_{\rm Si} = 4000\,{\rm S/m}$.

To explore how the absorption is generated, we simulate the distributions of surface current of the MM absorber at 0.67 and 1.63 THz, as shown in Fig. 3. From Fig. 3(a), we can see the calculated surface current density provides a simple way to visualize the absence of a magnetic response. A clockwise and counterclockwise circulating surface currents in adjacent metallic split-ring resonators cancel the magnetic fields. This means that the metallic split-ring resonators characterized in the present study exhibit a resonant response to the electric field while minimizing or eliminating any response to the magnetic field at the lower frequency of 0.67 THz for $\sigma_{\rm Si} = 1\,{\rm S/m}$. From Figs. 3(a) and 3(b), we can see that the magnetic component of the incident THz wave penetrates between the top and bottom layers and generates antiparallel surface current on the metallic split-ring resonators and the ground metal plane, leading to the magnetic coupling and the response. It is indicated that the absorption originates from the electric response of the top rings and the magnetic response between the two layers at the lower frequency of 0.67 THz without illumination. With increasing photoconductivity of silicon, the resonance absorption initially weakens and it starts to shift to higher frequencies. Finally, for $\sigma_{\rm Si} = 4000\,{\rm S/m}$, its linewidth broadens and the resonance absorption can reach 100% at 1.63 THz. Therefore, a fairly broad blueshift, as much as 59%, has been achieved requiring a lower photoconductivity. The low frequency resonant absorption associated with the circulating surface currents in outside of the two metallic split-ring resonators is nearly entirely quenched. The inner two metallic bars work as a dipole for higher-frequency absorption as shown in Fig. 3(c). The broadening of high frequency resonant absorption is mainly determined by enhanced dipolar coupling. It should be noted (Figs. 3(c) and 3(d)) that resonance currents are also anti-parallel in the metallic split-ring resonators and the ground metal plane, which is the basis of the magnetic response. The MM absorber interacts with the incident electromagnetic field for an electric resonator and a magnetic resonator in this way and exhibits high energy absorption. Therefore, a low conductivity of photoconductivity of silicon is required to completely switch off the mode of the resonant absorption.

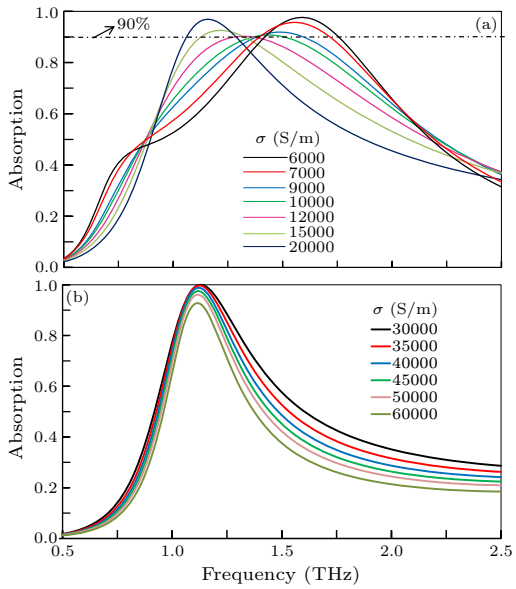

Fig. 4. Simulated absorption spectrum of the proposed MM absorber for different values of silicon conductivity.

With photoconductivity of silicon further increases (6000–20000 S/m), as plotted in Fig. 4(a), the absorber frequency can be continuously tuned from 1.60 THz to 1.16 THz, a redshift tuning range of 28%. Finally, the resonant absorption frequency tends to be stable at about 1.12 THz, while the absorption strength has a merely tiny decrease and keeps above 93% when the conductivity becomes larger (30000–60000 S/m) as shown in Fig. 4(b). The SRR can be thought of as an LC resonator with a resonance frequency of $\omega = (LC)^{-1/2}$, where the inductance results from the current path of the SRR and capacitance is mainly determined by the split gap. Any change in the capacitance or the inductance will shift the resonance frequency, making MM absorber sensitive to the lo-

cal environment. As the conductivity increases, much more charges accumulate at the edge of the silicon plates, which increases the capacitance, and therefore leads to shift to a lower frequency. At high conductivity values above 20000 S/m, the silicon begins to behave more like a metal and to allow the surface current through the split gap, and does not provide appreciable capacitive response.

We also explore the polarization properties and dependence of absorption on the incident angle for transverse electric polarization waves. Thanks to the orthogonal symmetry of the proposed metamaterial absorber in x–y plane, this metamaterial absorber can work for incident EM waves with all polarizations. The proposed metamaterial absorber is insensitive to the polarization angle of the incident waves.

In summary, we have demonstrated an optically controlled broadband blueshift and redshift of a terahertz switchable MM absorber, whose element is based on incorporation of photoconductive silicon in the critical region. The absorptive frequencies of the MM can be shifted by changing the intensity of an external light source. It is important that we have demonstrated a resonance absorption firstly shift to higher frequencies and then to lower frequencies until tending to be stable. The design incorporating semiconductors in critical regions of metallic split-ring resonators are more amenable to fabrication and also offer greater flexibility in applications of MM devices in any frequency range, which also benefits THz applications. Future technologies will push for a further step in applications of frequency-agile devices and the construction of future novel devices.

References

[1] Chen H T, Padilla W J, Zide J M O, Gossard A C, Taylor A J and Averitt R D 2006 *Nature* **444** 597
[2] Chen H T, O'Hara J F, Azad A K, Taylor A J, Averitt R D, Shrekenhamer D B and Padilla W J 2008 *Nat. Photon.* **2** 295
[3] Tao H, Landy N I, Bingham C M, Zhang X, Averitt R D and Padilla W J 2008 *Opt. Express* **16** 7181
[4] Iwaszczuk K, Strikwerda A C, Fan K, Zhang X, Averitt R D and Jepsen P U 2012 *Opt. Express* **20** 635
[5] Ferguson B and Zhang X C 2002 *Nat. Mater.* **1** 26
[6] Tonouchi M 2007 *Nat. Photon.* **1** 97
[7] O'Hara J F et al 2008 *Opt. Express* **16** 1786
[8] Chiang Y J, Yang C S, Yang Y H, Pan C L and Yen T J 2011 *Appl. Phys. Lett.* **99** 191909
[9] Hao J, Wang J, Liu X, Padilla W J, Zhou L and Qiu M 2010 *Appl. Phys. Lett.* **96** 251104
[10] Ma Y, Chen Q, Grant J, Saha S C, Khalid A and Smith D R 2011 *Opt. Lett.* **36** 945
[11] Shrekenhamer D, Xu W, Venkatesh S, Schurig D, Sonkusale S and Padilla W J 2012 *Phys. Rev. Lett.* **109** 177401
[12] Landy N I, Sajuyibge S, Mock J J, Smith D R and Padilla W J 2008 *Phys. Rev. Lett.* **100** 207402
[13] Shen X P, Cui T J, Zhao J, Ma H F, Jiang W X and L I H 2011 *Opt. Express* **19** 9401
[14] Wen Q Y, Zhang H W, Xie Y S, Yang Q H and Liu Y L 2009 *Appl. Phys. Lett.* **95** 241111
[15] Xiong H, Hong J S, Luo C M and Zhong L L 2013 *J. Appl. Phys.* **114** 064109
[16] Shen Z Y, Huang X J, Yang H L, Xiang T Y, Wang C W, Yu Z T and Wu J 2018 *J. Appl. Phys.* **123** 225106
[17] Xu Z C, Gao R M, Ding C F, Zhang Y T and Yao J Q 2014 *Chin. Phys. Lett.* **31** 054205
[18] Li S X, Nugraha P S, Su X Q, Chen X Y, Yang Q L, Unferdorben M, Kovács F, Kunsági-Máté S, Liu M, Zhang X Q, Ouyang C M, Li Y F, Fülöp J A, Han J G and Zhang W L 2019 *Opt. Express* **27** 2317
[19] Li Y J, Wang C W, Shen Z Y, Wu D, Wu N and Yang H L 2019 *Phys. Scr.* **94** 035703
[20] Li Y J, Huang X J, Huang S Q, Zhou Y F, Wu J, Wang C W, Shen Z Y and Yang H L 2019 *Mater. Res. Express* **6** 085806
[21] Lee S H, Choi M, Kim T T, Lee S, Liu M, Yin X, Choi H K, Lee S S, Choi C G, Choi S Y, Zhang X and Min B 2012 *Nat. Mater.* **11** 936
[22] Yan R, Sensale-Rodriguez B, Liu L, Jena D and Xing H G 2012 *Opt. Express* **20** 28664
[23] Mousavi S H, Kholmanov I, Alici K B, Purtseladze D, Arju N, Tatar K, Fozdar D Y, Suk J W, Hao Y, Khanikaev A B, Ruoff R S and Shvets G 2013 *Nano Lett.* **13** 1111
[24] Yao Y, Kats M A, Genevet P, Yu N, Song Y, Kong J and Capasso F 2013 *Nano Lett.* **13** 1257
[25] Driscoll T, Kim H T, Chae B G, Kim B G, Lee Y W, Jokerst N M, Palit S, Smith D R, Ventra M D and Basov D N 2009 *Science* **325** 1518
[26] Zhang Z, Tian Z, Chang C, Wang X G, Zhang X Q, Quyang C M, Gu J Q and Zhang W L 2018 *Nanotechnology and Precision Engineering* **1** 123
[27] Wen Q Y, Zhang H W, Yang Q H, Xie Y S, Chen K and Liu Y L 2010 *Appl. Phys. Lett.* **97** 021111
[28] Wen Q Y, Zhang H W, Yang Q H, Chen Z, Long Y, Jing Y L, Lin Y and Zhang P X 2012 *J. Phys. D* **45** 235106
[29] Shen N H, Kafesaki M, Koschny T, Zhang L, Economou E N and Soukoulis C M 2009 *Phys. Rev. B* **79** 161102
[30] Liu S, Zhang L, Yang Q L, Xu Q, Yang Y, Noor A, Zhang Q, Iqbal S, Wang X, Tian Z, Tang W X, Cheng Q, Han J G, Zhang W L and Cui T J 2016 *Adv. Opt. Mater.* **4** 1965
[31] Yan X, Liang L J, Zhang Z, Yang M S, Wei D Q, Wang M, Li Y P, Lv Y Y, Zhang X F, Ding X and Yao J Q 2018 *Acta Phys. Sin.* **67** 118102
[32] Xu Z C, Gao R M, Ding C F, Wu L, Zhang Y T and Yao J Q 2015 *Opt. Mater.* **42** 148
[33] Xu Z C, Gao R M, Ding C F, Wu L, Zhang Y T and Yao J Q 2015 *Opt. Commun.* **344** 125
[34] Hu T, Bingham C M, Strikwerda A C, Pilon D, Shrekenhamer D, Landy N I, Fan K, Zhang X, Padilla W J and Averitt R D 2008 *Phys. Rev. B* **78** 241103